Weldon School of Biomedical Engineering Faculty
Publications

Weldon School of Biomedical Engineering

1991

Design and evaluation of closed-loop feedback control of minimum temperatures in human intracranial tumors treated with interstitial hyperthermia

J A. Deford

Charles F. Babbs
Purdue University, babbs@purdue.edu

U H. Patel

N E. Fearnot

J A. Marchosky

See next page for additional authors

Recommended Citation

Authors

J A. Deford, Charles F. Babbs, U H. Patel, N E. Fearnot, J A. Marchosky, and C J. Moran

Design and evaluation of closed-loop feedback control of minimum temperatures in human intracranial tumors treated with interstitial hyperthermia

J. A. DEFORD[1], C. F. BABBS[1], U. H. PATEL[1],
N. E. FEARNOT[2], J. A. MARCHOSKY[3] and C. J. MORAN[4]

1. Biomedical Engineering Center, Purdue University, West Lafayette, Indiana, USA.
2. MED Institute, Inc., West Lafayette, Indiana, USA
3. Neurosurgical Associates, Chesterfield, Missouri, USA
4. Radiological Associates, Chesterfield, Missouri, USA

Abstract—The dynamic nature of blood flow during hyperthermia therapy has made the control of minimum tumor temperature a difficult task. This paper presents initial studies of a novel approach to closed-loop control of local minimum tissue temperatures utilizing a newly developed estimation algorithm for use with conductive interstitial heating systems. The local minimum tumor temperature is explicitly estimated from the power required to maintain each member of an array of electrically heated catheters at a known temperature, in conjunction with a new bioheat equation-based algorithm to predict the 'droop' or fractional decline in tissue temperature between heated catheters. A closed loop controller utilizes the estimated minimum temperature near each catheter as a feedback parameter, which reflects variations in local blood flow. In response the controller alters delivered power to each catheter to compensate for changes in blood flow. The validity and stability of this estimation/control scheme were tested in computer simulations and in closed-loop control of nine patient treatments. The average estimation error from patient data analysis of 21 sites at which temperature was independently measured (three per patient) was 0.0 ^{o}C, with a standard deviation of 0.8 ^{o}C. These results suggest that estimation of local minimum temperature and feedback control of power delivery can be employed effectively during conductive interstitial heat therapy of intracranial tumors in man.

1 Introduction

The clinical use of local heat therapy for the treatment of malignant disease has gained increasing visibility as a possible fourth modality of cancer therapy. Many clinicians have reported cases in which conventional therapies of surgery, radiation, or chemotherapy had failed; yet heat alone or heat in conjunction with conventional therapies demonstrated dramatic tumor regression (CRILE, 1962; LEVEEN et al., 1976; 1980; STORM et al., 1979). Yet, despite recent advances in equipment, technology, and techniques for treating malignant tumors with hyperthermia, the clinical results have remained disturbingly inconsistent (PEREZ et al., 1988).

The predominant reasons for failure of current hyperthermia therapies, as demonstrated in a large multi-center study (PEREZ et al., 1988), would appear to be

  a) the lack of accurate knowledge about tumor temperature distributions
  b) the absence of precise control of tumor temperature distributions, which can vary widely
  c) the presence of under-heated volumes, or cold spots.

These interrelated difficulties stem from an underlying lack of knowledge about tissue temperatures. The knowledge of temperature distributions during treatment is limited to a small number of implanted temperature sensors located at discrete sites. In the light of classical studies (CETAS et al., 1980; DEWHIRST et al., 1984) showing the minimum intratumoral temperature to be a highly correlated indicator of the efficacy of heat treatments in animals, it was our conclusion that human clinical results have probably been inconsistent because the tissue temperature elevations have been inconsistent. Accordingly, it has been .our goal to develop a system to determine and control, online and in real time, the minimum tissue temperature in a defined patient population receiving hyperthermia therapy for malignancy. This paper describes the solution of this control problem for the case of a conceptually simple, conductive interstitial technique. The solution allows online control of local minimum tumor temperatures throughout the treatment volume, even in the presence of time-varying blood flow.

The conductive interstitial modality employs an array of 2.2 mm diameter interstitially implanted catheters (BAUMANN and ZUMWALT, 1989). The catheters contain electrically resistive heating elements and are implanted directly into intracranial tumors by a neurosurgeon. The geometry of the implantation is controlled using a template to specify the location of burr holes to be drilled through the skull (BAUMANN and ZUMWALT, 1989). The catheters are implanted such that each is equidistant from its six nearest neighbors, forming a pattern of equilateral triangles (Fig. 1). To maximize the delivered energy to the tumor and to minimize the energy delivered to adjacent normal tissue, the heating element length within the implanted catheter can be specified (2-8 cm) and thus tailored to tumor diameter, previously estimated from computed tomographic (CT) scans (BAUMANN and ZUMWALT, 1989).
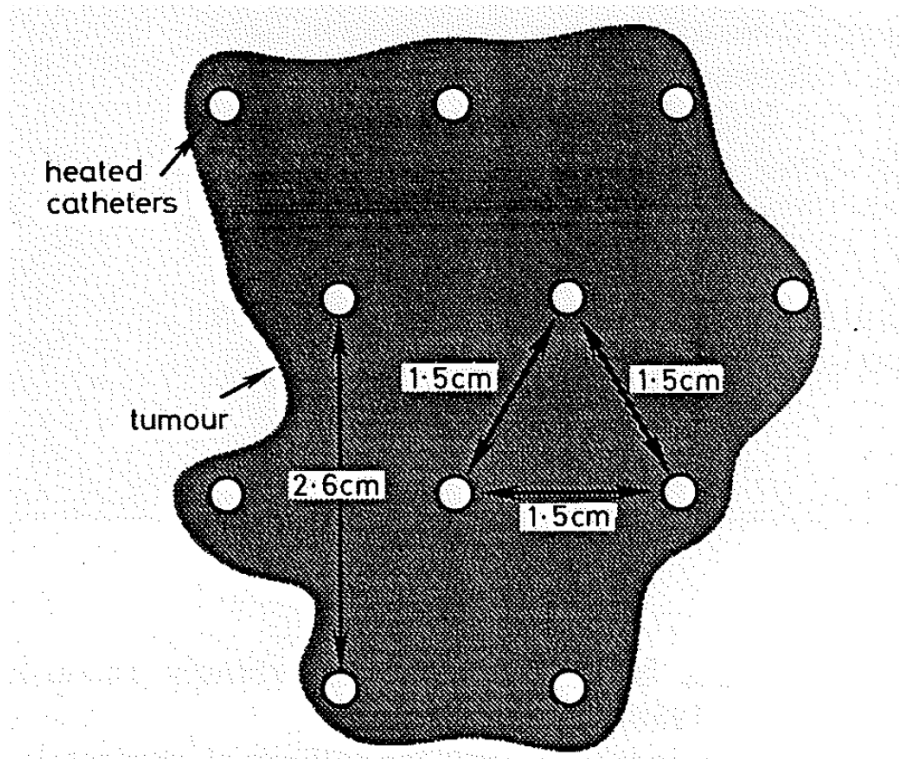
Fig. 1 Heating catheter implantation geometry as seen in cross section. Each triplet of catheters forms an equilateral triangle with 15mm sides or inter-catheter spacing. The heating catheters are 2.2 mm in diameter.

Application of electric current to each resistive element converts electric energy directly to heat. The heated catheter, in turn, warms the tissue nearby through thermal conduction and, to some extent, by the bulk flow of blood within the tumor. Each catheter contains a temperature sensor (thermistor) that is located in the center of the catheter in contact with the internal heating element to monitor its temperature, which can be adjusted under computer control. The relevant physics of heat transfer are similar in concept to those of inductively heated ferromagnetic thermoseeds (OLESON and CETAS, 1982). The potential for achieving computer aided, closed loop control of tissue temperatures is much greater with electrically heated catheters than with other hot source techniques, because each catheter is electrically heated and activated.
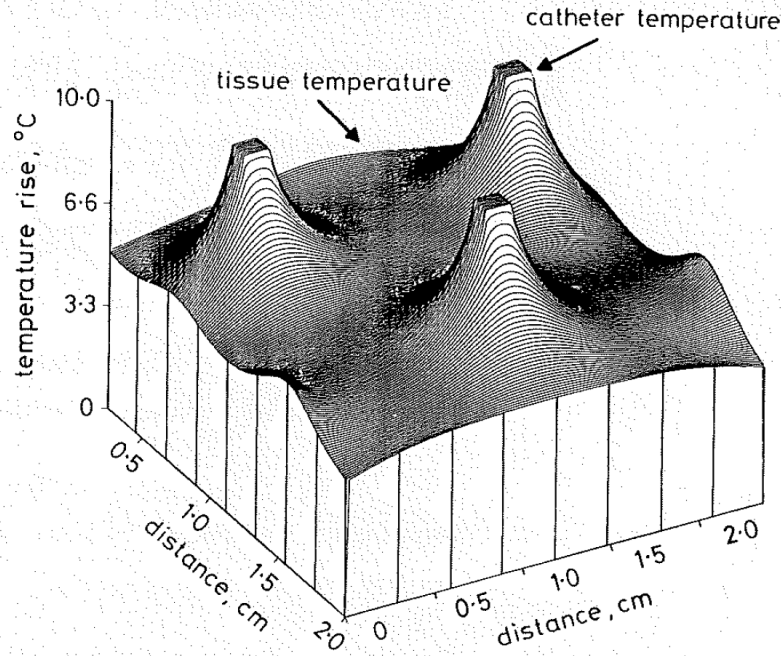
Fig. 2 The temperature distribution between a triplet of heated catheters will assume the presented form. The warmest area or temperature peak occurs in the center of a heating catheter, while the coolest area or temperature valley occurs in the center of the triplet. Zero represents the level of baseline arterial temperature. Here cylindrical catheters are modeled as rectangular solids for simplicity, causing square profiles of the thermal peaks. Catheter power is 100 mW/cm and blood flow is 10 ml/min/100 g.

When the heated catheters are implanted in arrays with a nominal 15 mm inter-catheter spacing and triangular symmetry, the temperature profile near a triplet of catheters assumes the form presented in Fig. 2. A fundamental feature of the temperature profile can be described by a dimensionless parameter that we call thermal 'droop'. The droop is defined, when inter-catheter spacing is small compared with the length of the heating element, as the fractional decline in tissue temperature between neighboring heated sources and can assume a value between zero and unity; specifically

$$\text{droop} = \frac{T_{catheter} - T_{minimum}}{T_{catheter} - T_{arterial}}. \tag{1}$$

A droop of zero indicates that the local minimum tissue temperature equals the nearby source (catheter) temperature. This value could only occur if there is zero blood flow through the heated region. A droop of unity indicates that the local minimum tissue temperature is equal to arterial or core body temperature. This value would occur in the presence of extremely high blood flow or extremely wide catheter spacing. Thus, droop is a dimensionless, normalized descriptor of

4

local minimum tumor temperature, defined for the particular case of staggered arrays of conductive interstitial catheters.

If one rearranges Equation (1), solving for the local minimum tissue temperature $T_{minimum}$, the result,

$$T_{minimum} = T_{catheter} - droop(T_{catheter} - T_{arterial}),$$
(2)

provides an expression for local minimum tissue temperature as a function of catheter temperature, arterial (or core body) temperature, and droop. The problem of finding an online estimator of local minimum tumor temperature reduces to finding an online method of calculating droop, in conjunction with catheter temperature and arterial (or core body) temperature, both of which are easily measured.

Once a method of determining droop is developed, it is then possible to incorporate closed-loop control using the estimated minimum temperature as a local feedback parameter for independent control of each heating element. Earlier work had suggested that droop can be accurately estimated from the steady-state catheter power and the temperature for at least some cases of conductive interstitial heat therapy. This approach seemed to be workable and attractive. Hence, the goals of the present study were to

  a) develop a system to control local minimum tissue temperatures based upon the 'droop' estimator of local minimum temperature
  b) assess the stability of the estimation/control system
  c) implement the system in a clinical setting.

2 Methods

2.1 Bioheat transfer equation

To determine an estimator for thermal droop during conductive interstitial hyperthermia we employed the bioheat transfer equation of PENNES (1948). For a control volume of tissue small enough so that all the thermal properties within it can be considered constants, the bioheat transfer equation may be written as

$$\dot{q}_{met} + P + K\nabla^2 T + c_b\omega_b(T_b - T) = \rho c \frac{\partial T}{\partial t},$$
(3)

where q_{met} is the specific rate of metabolic heat production, which is negligible in the context of local heat therapy for cancer, P is the power density delivered to tissue, which is zero for the conductive interstitial modality, K is the tissue thermal conductivity, T is the temperature of tissue, c_b is the specific heat of blood, ω_b is the specific flow rate of blood in capillaries, T_b, is the temperature of blood, ρ is the mass density of tissue, c is the specific heat of tissue, and t is time. Equation (3) governs both transient and steady-state heat transfer. In the steady-state case,

which develops for the conductive interstitial modality after about five to ten minutes, $\frac{\partial T}{\partial t} = 0$, and the equation simplifies to

$$KV^2T + c_b\omega_b(T_b - T) = 0.$$ (4)

Literature values were used for brain tissue thermal conductivity (0.5275 W/(m ^{o}C) (COOPER and TREZEK, 1971) and blood specific heat (3642.6 J/(kg ^{o}C) (ALBRITTON, 1952). Further details of the computational methods used to solve this form of the bioheat equation are presented elsewhere (DEFORD et al., 1990).

2.2 Local minimum temperature estimation

To estimate droop, and in turn, local minimum temperatures, the bioheat transfer equation was utilized to characterize droop as a function of clinically measurable variables. Using the computer models previously described (DEFORD et al., 1990), we performed many simulations for arrays of heated catheters in tissue supplied by perfusions from 0 to 100 ml/min/100 g. Catheter powers ranged from 0 to 0.4 W/cm of catheter length. From simulation parameters and Equation (1) we found that droop was a simple, computable function of catheter power and catheter temperature, given a fixed inter-catheter spacing (Fig. 3). Noting that each curve in Fig. 3 has a similar shape, a simple normalization was then found. After dividing the power per unit length delivered to a catheter by its temperature rise above arterial temperature, the curves collapsed to a single curve (Fig. 4). Performing a second-order polynomial regression of the curve in Fig. 4, we then obtained an estimation equation for droop as a function of the clinically measurable parameters: catheter temperature, catheter power, and arterial blood or core body temperature.
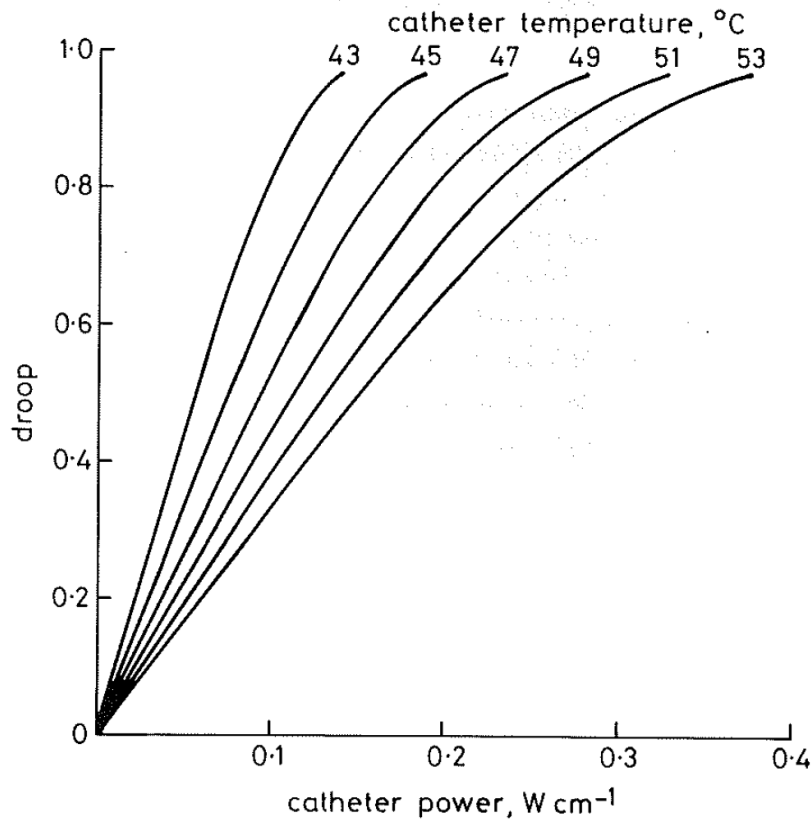
Fig. 3 Droop is a polynomial function of heating catheter temperature and steady-state power per unit length. Note that a unique curve exists for each value of internal heating catheter temperature.

This estimation equation is presented in terms of a normalized power, σ, (catheter power/heating element length/catheter temperature rise) in W/cm/$^\circ$C for interior catheters in an array with 15 mm spacing, namely

$$\text{droop} = a + b\sigma + c\sigma^2 \tag{5}$$

where a= -0.0057, b=75.2 cm$^\circ$C/W , and c= -861.7 (cm$^\circ$C/W)^2 for the case of 15 mm inter-catheter spacing (Fig. 1). Similar functions exist for other catheter spacings, but they are not at present used clinically. All the factors required to calculate σ -- catheter power per unit length and internal temperature rise -- are readily available from hardware driving commercially available electrically heated catheters (Cook Inc., Bloomington, Indiana, USA).

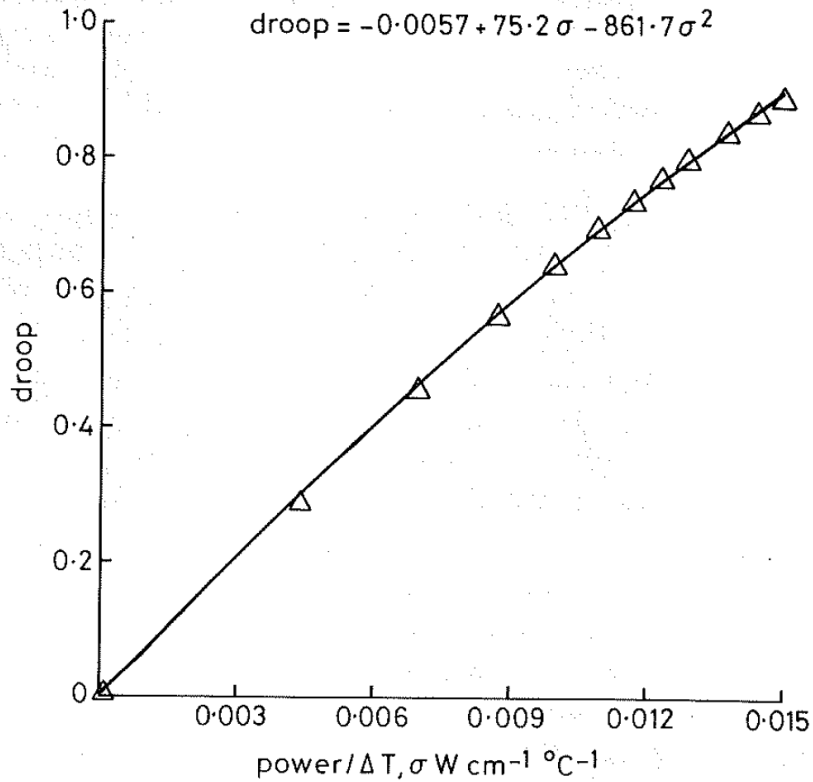$$\text{droop} = -0.0057 + 75.2\,\sigma - 861.7\sigma^2$$

Fig. 4 If the delivered power per unit length to the heating catheter is divided by the resultant internal catheter temperature rise (above arterial temperature), the multiple curves of Fig. 3, for 15 mm catheter spacing, collapse to a single polynomial function. Performing a second-order regression of the resultant curve allows the development of an estimation equation for droop as a function of internal heating catheter temperature and power per unit length.

Substitution of Equation (5) for droop in Equation (2) provides a simple, rapidly computable expression

$$T_{minimum} = T_{catheter} - \left(a + b\sigma + c\sigma^2\right)\left(T_{catheter} - T_{arterial}\right), \tag{6}$$

which allows the estimation of local minimum intratumoral temperature near each implanted catheter.

The estimation Equation (5) was determined from multiple computer simulations of the bioheat Equation (4), which describes the steady-state behavior of heat transfer in biological tissue. Steady-state conditions exist, approximately, for most of the duration of the treatment. In the control problem we are also concerned with the transient (heat up) phase of the catheter-tissue system (lasting about 10 min). We must be assured that the temperature estimate, derived from Equation (6), at least tracks the true tissue temperature during the transient heat-up phase to

8

ensure a stable and accurate estimation/control system at these early times. A plot of the response of the catheter/tissue system to a step input in power in computer simulations (Fig. 5) demonstrates the difference between bioheat equation-determined local minimum temperatures and those estimated from Equation (6). The greatest difference between the two temperature curves appears when the slopes of the curves are maximum, as predicted from Equations (3) and (4). Although the two curves are not identical, the estimation is a good approximation to the bioheat equation-determined minimum tissue temperature curve, with the same curve shape and timing. Estimated temperature from Equation (5) was accordingly selected as a practical feedback control parameter, for both the initial heat-up phase and for the more nearly steady-state phase.
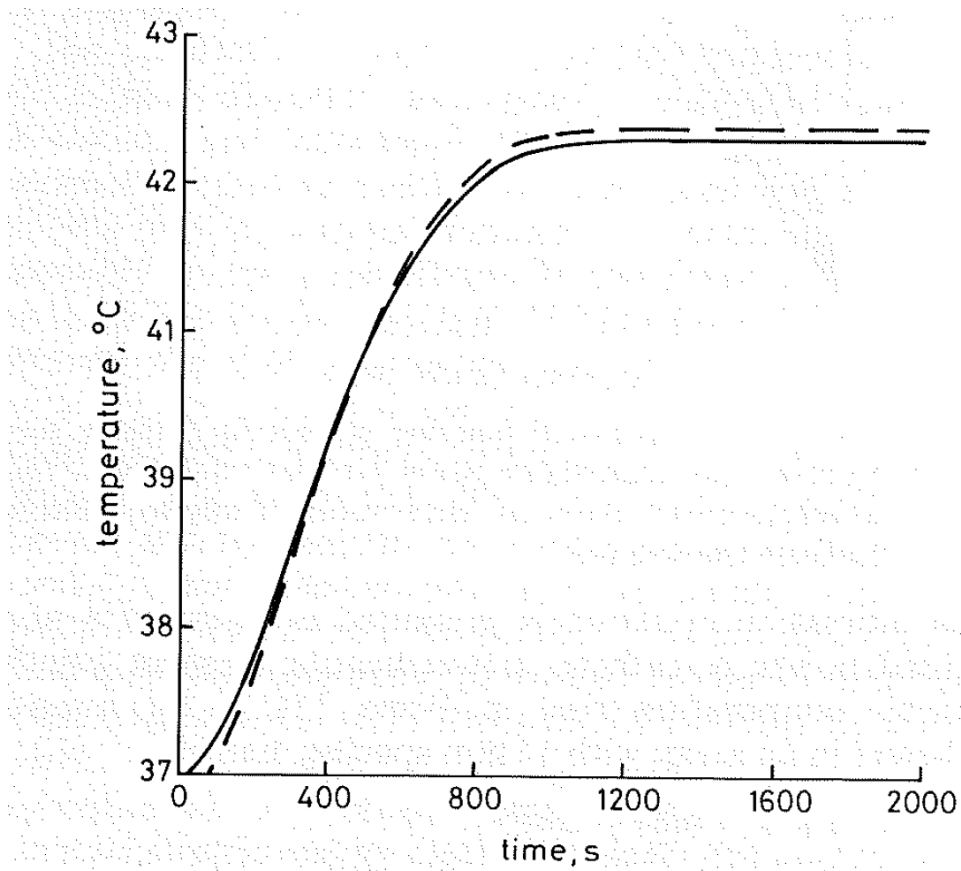

Fig. 5 A step input of 160 mW/cm to a each heating catheter (surrounded by similar heating catheters) and given a local perfusion of 20 ml/min/100 g yields the minimum temperature step response for both the bioheat equation and the minimum temperature estimation equation, based upon ordinary differential equations. There is little difference between the two temperature curves, demonstrating the accuracy of the estimation equation even during transient heating. The baseline arterial temperature was 37 ^{o}C.

2.3 Stability of the controller design

Development of the estimation Equation (6) appears to provide a route to feedback control of local minimum temperatures. Evaluation of control system stability was necessary before such a controller could be responsibly implemented in patient treatments. The bioheat transfer equation is an accurate model of tissue heat transfer (CHARNY and LEVIN, 1988; CLEGG and ROEMER, 1985; PANTAZATOS and CHEN, 1978), and is described in terms of partial differential equations (PDEs). In the context of current control theory, this poses a difficult problem. Tools to aid in the design and stability analysis of controllers for systems described by PDE's are very limited and may only be used in very specific cases (OGATA, 1970). However, because any estimation/control system for hyperthermia therapy will be employed in the treatment of human patients, it must be unconditionally stable. To further confound the problem, the system we seek to control is dynamic, i.e. time varying, because blood flow is time varying. Therefore, to design and evaluate a safe and effective control system using the conceptual tools presently available, an ordinary differential equation model (ODE) is highly desirable.

Analysis of tissue temperature responses to step and sinusoidal power inputs to the various bioheat equation models allowed the identification of simple, linear ODE models that closely mimicked the transient response of local minimum tissue temperature, as described by the complete bioheat equation and Equation (6). It was discovered that the dominant mode (or time constant for the ODE model) of the system varied with blood flow as can be seen in Fig. 6. The dominant tissue mode or time constant varied from 45 sec for high blood flows (100 ml/min/100 g) to over 2000 sec for very low blood flows (1 ml/min/100 g) (Fig. 6). It was also evident that the system gain (tissue temperature rise/input power) also varied with blood flow. The system gain increased from almost zero to about 25°C/W as blood flow varied from 100 down to 1 ml/min/100 g. Because there is a physical separation between the hot source (catheter) and the location of the minimum temperature (about 8-9 mm from the source with 15 mm catheter spacing), there is a time delay between the application of a step change in catheter power and a temperature rise at a central location between catheters. This delay, found from computer simulations, was about 45 sec, regardless of the blood perfusion rate.
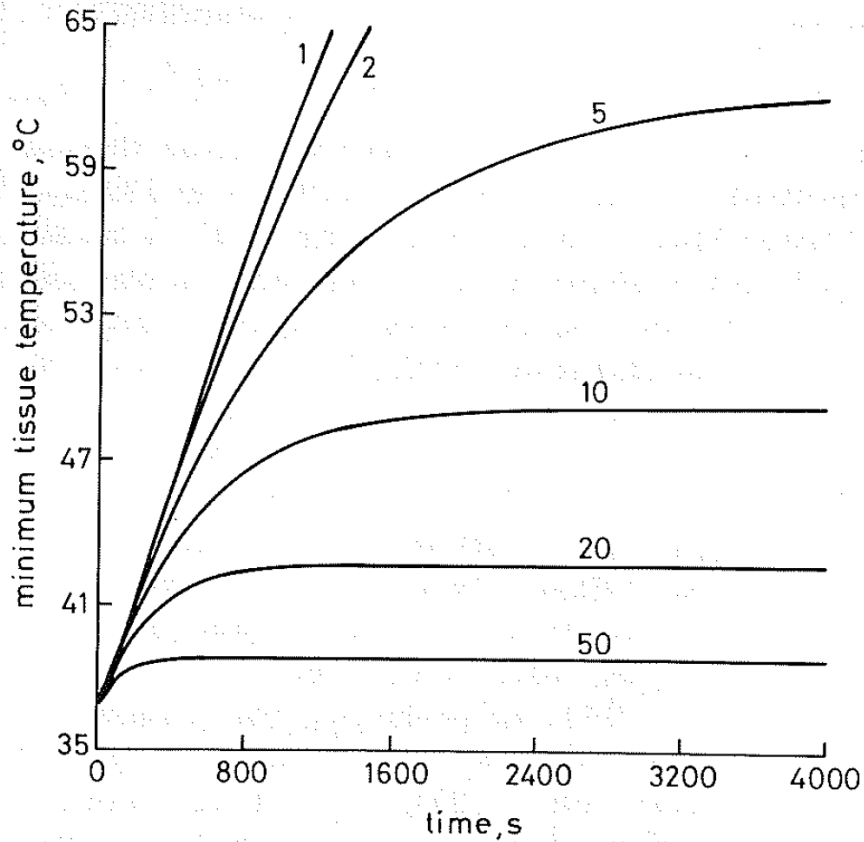
Fig. 6 Given a step input of 160 mW/cm to each heating catheter (surrounded by similar heating catheters) in the presence of local perfusion ranging from 1 ml/min/100 g to 50 ml/min/100g yields the multiple minimum temperature responses. As blood flow increases the step response time decreases, and the steady-state value of the minimum temperature decreases. The baseline arterial temperature was 37 °C.

The results of the step and sinusoidal simulations allowed the development of a family of first-order ODE models to describe tissue heating; a different model for each blood flow. A classical transformation technique (the Laplace transform) relating time functions to frequency dependent functions of a complex variable, s , was used to analyze this control problem (OGATA, 1970). Laplace transform techniques are used extensively throughout the remainder of this manuscript. The application of the Laplace transform replaces functions of time by a complex function dependent upon frequency (OGATA, 1970). The variable s is defined as $\phi + j\omega$. where ϕ and ω are real variables, and $j = \sqrt{-1}$. Employing the Laplace transform and standard methods for finding the inverse Laplace transform, the transient behavior of the bioheat equation can be emulated by a family of first-order models with a single gain and single time constant. The general form of the model is

$$T_{tissue}(s) = \frac{Ke^{-\theta s}}{\tau s + 1},$$ (7)

where K is the open loop system gain (°C/W), τ is the system time constant (in sec), and θ is the system delay time (in sec). For a local perfusion of 1.0 ml/min/100 g, which might occur in the central regions of a large tumor, the first-order model in the s-plane is

$$T_{tissue}(s) = \frac{24.6e^{-4.5s}}{2570s + 1};$$ (8)

whereas a perfusion of 20 ml/min/100 g, which represents a typical tumor blood flow (PETERSON, 1979), leads to an ODE model of

$$T_{tissue}(s) = \frac{1.1e^{-4.5s}}{250s + 1}.$$ (9)

Table 1 presents the dependence of the open-loop gain, and the open-loop time constant on perfusion. Equations (7), (8) and (9) thus represent a set of perfusion-specific ODE models of a PDE (bioheat equation) governed system.

Table 1 First order gain and time constant (ODE for various blood flow rates)

Perfusion rate, $ml\,min^{-1}\,100\,g^{-1}$	Gain, $°C\,W^{-1}$	Time constant, s
1	24·6	2570
2	12·1	1550
5	4·6	960
10	2·3	507
20	1·1	250
30	0·67	165
40	0·46	123
50	0·35	97
60	0·27	79
70	0·22	67
80	0·18	57
90	0·15	50
100	0·12	43

Comparison of the ODE model response with the bioheat transfer equation (PDE) response demonstrated that the ODE models were good approximations to the system. Fig. 7 presents a step response of both the PDE and ODE models with a local perfusion of 10 ml/min/100 g. A good correlation exists between these models, adding confidence to our use of the ODE models. These ODE models could then be used to guide the development of the control system. The utility of these models does not require knowledge of the exact tissue perfusion in each particular case. Rather, the ODE models can serve as the basis for a worst-case analysis to design an unconditionally stable controller.
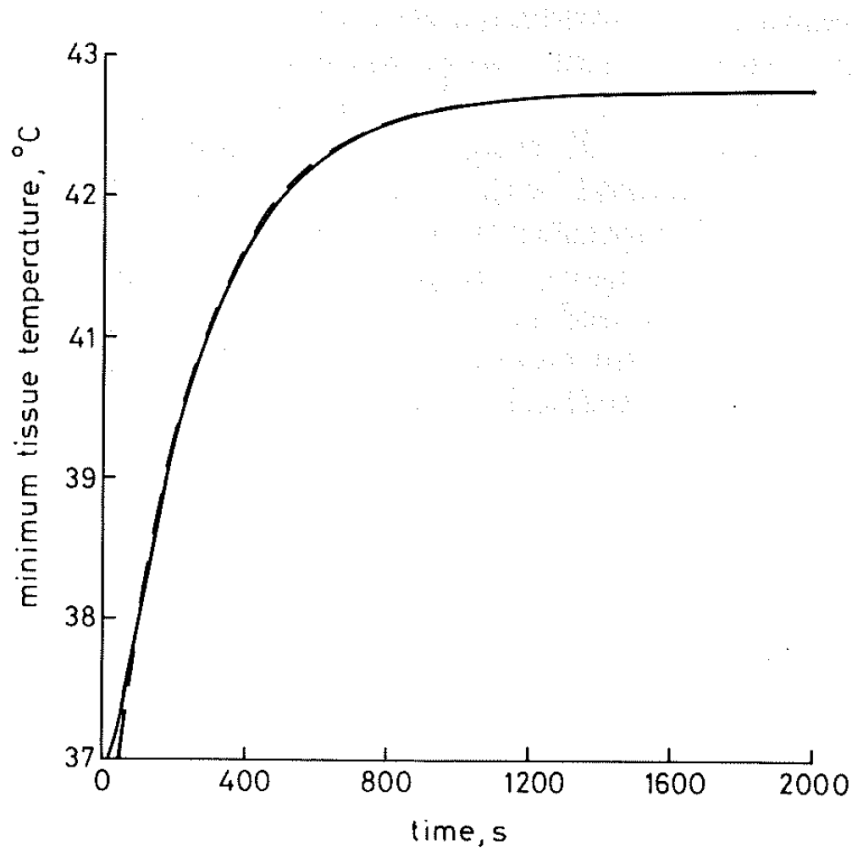

Fig. 7 Given a step input of 160 m W/cm to each heating catheter (surrounded by similar heating catheters) and a local blood flow of 20 ml/min/100 g yields the step response presented by the solid curve. Applying the same step input to the ODE model determined for a 20 ml/min/100 g blood flow yields the step response presented by the broken curve. The two curves are almost identical except for the small difference during the initial 100 sec. The baseline arterial temperature was 37°C. Solid curve represents bioheat equation (PDE). Dashed curve represents ODE model.

13

2.4 Practical aspects of controller design

To further simplify the engineering problem, the estimation/control system was initially developed for use with a single hyperthermia generation system, the VH8500 system (Cook, Inc., Bloomington, Indiana, USA). The specifications for this control system are as follows:

a) The system must be stable over the entire physiological range of blood flows (0-100 ml/min/100 g.
b) The system must simultaneously control multiple heating sources (currently up to 32 catheters).
c) It is desirable to have a rapid heat up to the pre-set point temperature (< 15min).
d) If any overshoot of the desired minimum temperature occurs, it must be minimal and short lived (< 3 ^{o}C for < 5 min).
e) The proposed system must operate without hardware modifications to the VH8500 hyperthermia generation system.

Since there exist many possible variations in system parameters, owing to its dynamic nature, the so-called optimal or state controllers (LUENBERGER, 1979) were ruled out as controller options. The VH8500 hyperthermia system utilizes an IBM XT compatible computer system for treatment planning, data storage, displaying graphics and treatment control. Therefore, a real limitation on the computational power exists. Considering the above specifications and limitations, we selected a proportional-integral (PI) control scheme (EL-HAWARY, 1984). The PI controller was also selected for its ability to control in the presence of system delays, nonlinearities, and transients that might exist during the course of actual hyperthermia treatment.

The proposed estimation/control system is displayed in block diagram form in Fig. 8. Disturbances (such as changes in local blood flow) would enter the system after the controller. Without feedback it would be impossible to compensate for disturbance effects. It would be desirable to feed back the actual local minimum temperature, and this would make the design of the control system much easier. However, all true local minimum temperatures cannot be obtained with current technology. The task would require implantation of an intolerably large number of temperature sensors. Therefore, the estimated minimum temperature was used as feedback. The estimate, from Equation (6), tracks local disturbances very well and is a good candidate for use as a feedback parameter.

Having selected the PI controller, control constants have to be determined that meet the presented specifications. Unconditional stability is of the foremost concern for this system, because equipment damage or patient injury is intolerable. Rather than using a classical definition of stability (OGATA, 1970) that would allow long-duration, high-amplitude damped oscillations, we specified a stability criterion that allowed a small overshoot of less than 3 °C and could last no more than 5 min. By these criteria, a decay ratio of greater than 0.75 was required. We defined the decay ratio as one minus the ratio of successive peaks or overshoots of the desired setpoint. Therefore, given a decay ratio of 0.75 the second peak (or overshoot) would be 25 per cent of the value of the first peak.
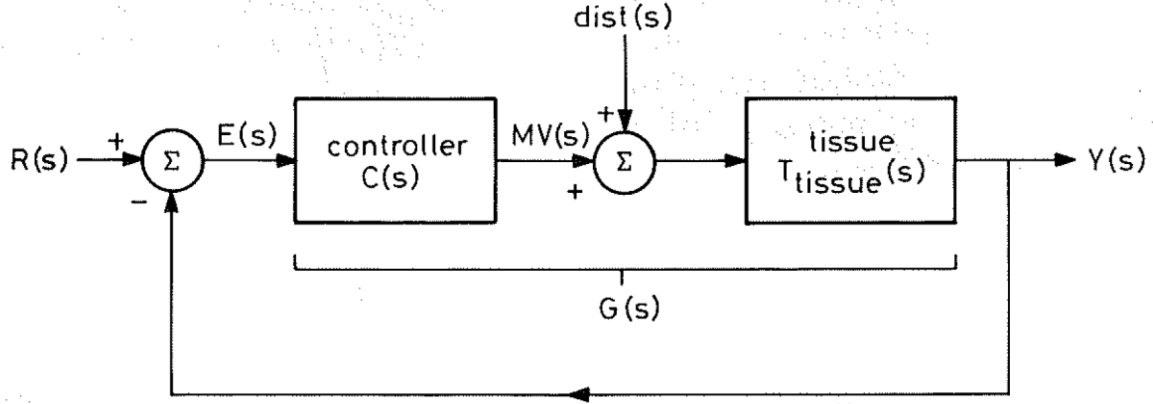
Fig. 8 The closed loop block diagram (in the s-domain) of the system model used in this study includes: R(s) =system input (minimum tissue temperature setpoint), E (s) = error between the estimated minimum temperature and the minimum temperature setpoint (Y(s)- R(s)), C(s) =controller used to map the error to an appropriate power intended to drive the error E(s) to zero, MV(s) =manipulated value or parameter varied by the controller (power delivered to the heating catheter), dist(s) = local disturbances such as changes in blood flow rates, $T_{tissue}(s)$ =ODE model of the local minimum tissue temperature, G(s) =a variable that lumps the controller and tissue model, used only to simplify notation, Y(s) =system output (minimum tissue temperature).

Utilizing the family of ODE models previously described (Table 1) a worst-case control situation was identified as the set of conditions that would most easily (with the smallest system disturbance) cause instability. At very low perfusions the system gain was the highest (≈ 25) and the dominant mode or time constant was the longest (≈ 2500 sec). These features, coupled with the long delay time (≈ 45 sec), as shown in Table 1, constitute a worst-case situation. If control parameters could be determined for this situation that meet all stability requirements, the same parameters could also be employed safely for other conditions, including all values of tissue blood flow > 1 ml/min/100 g. Employing the model presented by Equation (8) and the Laplace transform of the PI control law represented by

$$C(s) = K_P + \frac{K_1}{s},$$ (10)

where K_P is the proportional gain of the controller, K_1 is integration gain of the controller (EL-HAWARY, 1984), and s is again a complex frequency variable, yields the open loop system transfer function

$$G(s) = \left(K_P + \frac{K_1}{s} \right)\left(\frac{24.6e^{-4.5s}}{2570s+1} \right).$$ (11)

15

Rearranging Equation (10) as

$$C(s) = \frac{K_P}{s}(s+z),$$ (12)

where $z = (K_1/K_P)$, the open loop system input/output relationship, or transfer function, becomes

$$G(s) = \left(\frac{K_P}{s}(s+z)\right)\left(\frac{24.6e^{-4.5s}}{2570s+1}\right).$$ (13)

The closed loop system with unity gain negative feedback can be described as

$$\frac{Y(s)}{R(s)} = \frac{G(s)}{1+G(s)},$$ (14)

where $G(s)$ is the open loop system transfer function from Equation (13), $Y(s)$ is the system output (minimum tissue temperature), and $R(s)$ is the system input (minimum temperature setpoint) as presented in Fig. 8. The controller (Equation (10)) can be thought of as a system that transforms the error between the desired minimum temperature and the estimated minimum temperature to a power (the manipulated variable or MV) in order to drive the error to zero. Proper selection of controller constants K_P and K_1 was achieved by pole placement, using the root locus technique, such that the desired decay ratio > 0.75 was achieved. The root locus method (OGATA, 1970) was also used as an analysis tool to evaluate the stability of the closed-loop system.

The root locus is a method for finding the roots of the characteristic equation, where the characteristic equation is the denominator of a transfer function $(1 + G(s))$ from Equation (14) and the roots of this equation are the values of s that cause the characteristic equation to equal zero. Although the open-loop roots from Equation (13) are constants, when feedback is introduced and the gain varied, the closed loop roots become functions that may vary over a large range. To determine the system stability as the system gain changes (due to changes in blood flow) it is useful to know how the roots (or poles) of the closed loop system vary. A graphical representation of the roots can be drawn in the s-plane with real values of the roots along the abscissa and imaginary values along the ordinate. As all roots remain negative in sign, i.e. the root locus does not cross the imaginary axis (ordinate), the system is stable; at the point where the roots cross the imaginary axis the system is marginally stable, and all points to the right denote system instability (MARSHALL, 1979). Thus the left half-plane may be viewed as an area of negative feedback and the right half-plane as a positive feedback area. Fig. 9 presents the relationship between the root locus plots and time domain system stability. Notice that the system becomes more oscillatory as the roots (or poles) move away from the real axis (in the root locus) signifying the presence of complex valued roots. Crossing the imaginary axis denotes crossing from stability to instability.
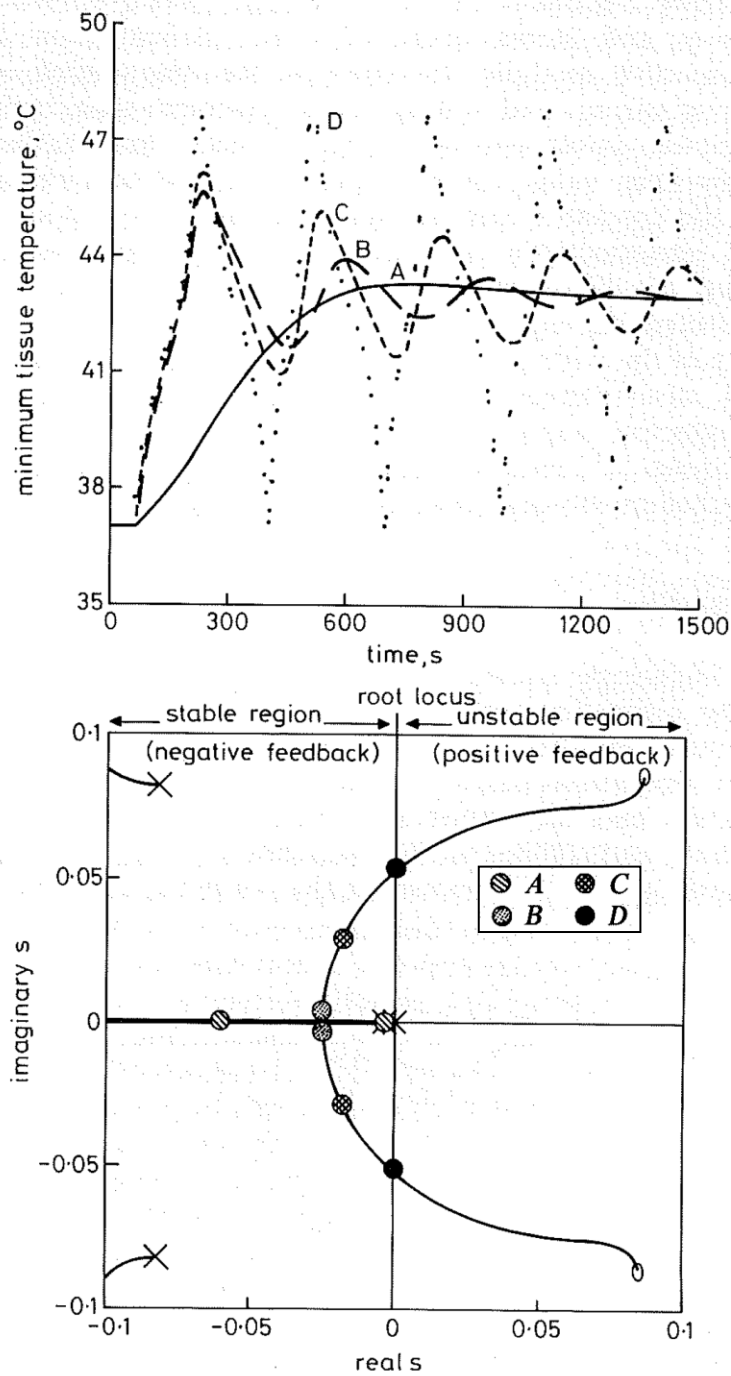
Fig. 9 The relationship between closed-loop stability and the root locus. Temperature curve A corresponds to points on the root locus labeled A and so forth. Note that the temperature curves become more oscillatory as the poles on the root locus (corresponding points) become complex and move away from the real axis, and instability (sustained oscillations) occurs when the poles cross to the right hand plane. The bold line on the real axis denotes the presence of the root locus.
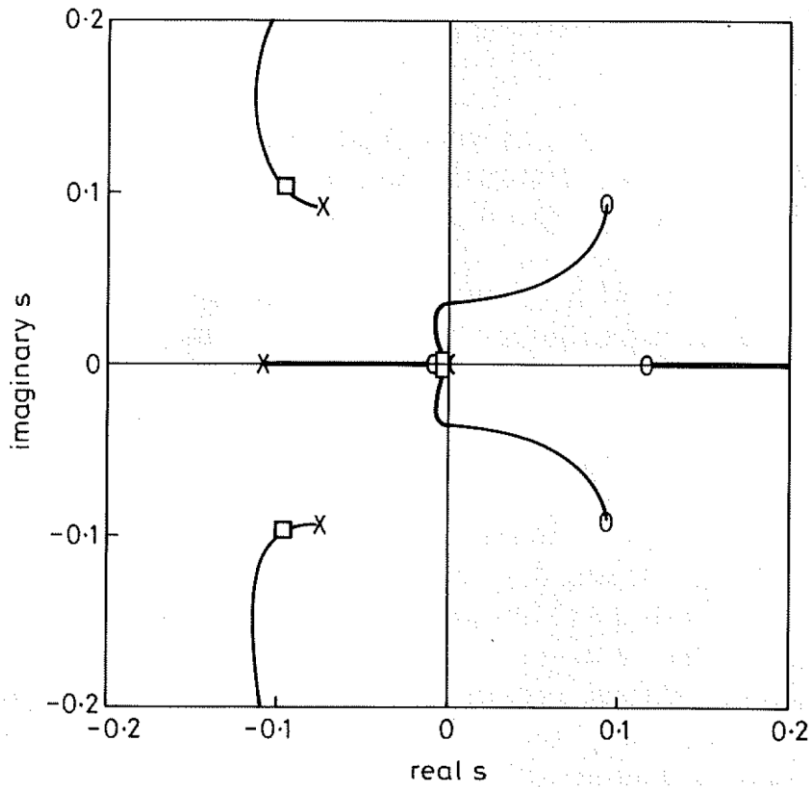
17

Fig. 10 The root locus of the closed loop system using the ODE tissue model for a blood flow of l ml/min/100 g. This was deemed the worst case, since the gain was high (24.6) and the time constant was long (2570 sec). The Xs denote open-loop poles and the Os denote open loop zeros of the system model presented in Equation (13). The boxes denote the location of the closed-loop poles using the presented PI controller (the operating point) with P = 0.608 and I = 200. As the boxes are on the left hand side of the imaginary axis, the closed loop system is stable. The bold lines denote the presence of the root locus on the real axis.

Figure 10 presents the root locus plot for the closed-loop system represented by Equation (13). The delay term, e^{-45s}, in Equation (12), is represented by a fourth-order Pade approximation (MARSHALL, 1979), indicated by the multiple poles in Fig. 10. The delay actually represents an infinite number of new poles added to the system (MARSHALL, 1979). From the root locus presented in Fig. 10, one may note that for a z of 0.003 (from Equation 11) the closed-loop system gain can range from zero to 48.5 still maintaining stability. For adequate damping we selected K_P as 0.608. Therefore, as z = 0.003, then K_1 must be 1/200.

18

Root loci were also generated to assess the stability of the closed loop system over the entire range of physiological blood flows (represented as the models that lie within the range of Equations (7) and (8)). Fig. 11 presents root loci for the 'best case' (represented by Equation 8), where best case implies the most rapid response to changes in setpoint or disturbances with minimal overshoot and no instability, while worst case (Equation (13) and Fig. 10) implies the converse. The root locus remains very near the real axis (abscissa) for the best case, demonstrating a very high decay ratio (i.e. little or no overshoot, and a rapid response). The root locus in the worst case begins to approach the imaginary axis (ordinate) with complex roots, but does not cross it, denoting a more oscillatory but stable response.
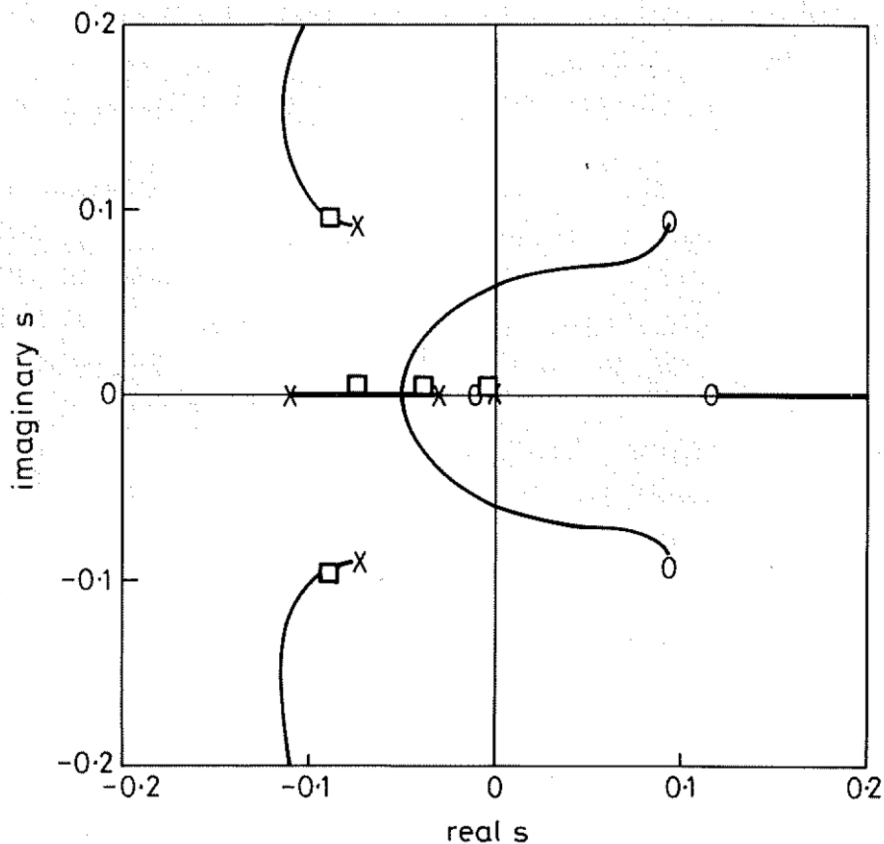

Fig. 11 The root locus of the closed loop system using the ODE tissue model for a blood flow of 100 ml/min/100 g. This was deemed the best case, because the gain was low (0.12) and the time constant was short (43 sec). The Xs denote the location of open-loop poles and the Os denote the location of open-loop zeros of the system model. The boxes denote the location of closed-loop poles using the PI controller with P = 0.608 and I= 200. Since the boxes are on the left hand side of the imaginary axis, the closed-loop system is stable. The bold lines denote the presence of the root locus on the real axis.

2.5 Clinical methods and data analysis

Having developed the worst-case controller based upon a defined family of linear ODE models, we tested the controller performance, first in computer simulations and then in clinical settings (Missouri Baptist Medical Center or St Luke's West Hospital, St Louis, Missouri, USA). The estimation/control system was first analyzed in computer simulations using the bioheat transfer equation. These simulations demonstrated that stability was maintained in the presence of a large step increase or a decrease in effective perfusion (step changes > 60 ml/min/100 g), thereby verifying that the estimation/control system could be used safely and effectively in the clinic.

To assess the validity and stability of the proposed system, eight patients were treated (one patient was treated twice) with the presented system. Each treatment was monitored to ensure system stability then retrospectively analyzed to determine the minimum temperature accuracy. Each patient was treated at Missouri Baptist Medical Center or St Luke's West Hospital in St Louis, Missouri, USA, with approval from their Institutional Review Boards (IRBs) and an investigational device exemption from the US Food & Drug Administration. There were six male and two female patients in this study, ranging in age from 41 to 67 years. The tumor types diagnosed at the time of hyperthermia treatment included four glioblastoma multiformes, three anaplastic astrocytomas and one metastatic lesion. The hyperthermia catheters were implanted as described previously (BAUMANN and ZUMWALT, 1989). The number of heating catheters implanted varied with tumor size and ranged from 6 to 17 with a median value of 11.

To monitor intratumoral temperatures between the implanted heat generating catheters, small diameter (1.2 mm) temperature sensing catheters (containing only thermistors) were implanted. The temperatures from these sensors were used as comparison values to determine the accuracy and stability of the estimation equation and controller. The General Electric 9800 CT scanner and computer were employed to determine the position of the heating and temperature sensing catheters. Sequential non-overlapping coronal CT scans with a slice thickness of 3 mm were obtained immediately after implantation; then, employing the CT computer, sagittal reconstructions were performed to measure the implantation geometry in cross section. Only those temperature sensing catheters that were within 3 mm of the center of a triplet of heating catheters were included in subsequent analysis.

During treatment the hyperthermia system (VH8500) acquires and stores operational and patient data for retrospective analysis. Included in the data stored are catheter current and voltage levels, treatment time, catheter power levels and individual catheter temperatures. Steady-state values of estimated minimum temperature and the corresponding measured minimum temperatures were retrospectively compared at multiple time instants during the three hour treatment. System stability was monitored during each patient treatment to ensure the safety of the patient. To study the occurrence and effect of local disturbances on the estimation/control system, retrospective analysis employing computer aided reconstructions of patient treatments were performed as described previously (DEFORD et al., 1990).

3 Results

3.1 Engineering studies

The estimation/control system was evaluated both in computer simulations and in the clinic. Results of computer simulations employing the transient bioheat transfer equation and the estimation/control system verified the accuracy and stability of the proposed system before clinical testing. Table 2 summarizes the simulated temperature estimation error, minimum temperature overshoot and the decay ratio for various local perfusions ranging from 1 ml/min/100 g to 100 ml/min/100 g (a much wider variation of blood flows than expected in patients). For each perfusion value tested over the above range, the estimation/control system proved to be accurate and stable--meeting or exceeding the design specifications.

Table 2 Closed-loop system performance as a function of local perfusion

Perfusion, $ml\,min^{-1}\,100\,g^{-1}$	Maximum overshoot, °C	Decay ratio d	Steady-state error, $T_{est} - T_{bio}$
1	2·8	0·79	0·0
2	2·4	0·79	0·0
5	1·9	0·85	0·1
10	1·1	0·96	0·1
20	0·3	0·97	0·0
30	0·04	0·97	0·1
40	0·002	0·99	0·1
50	0·0	1·0	0·0
60	0·0	1·0	0·0
70	0·0	1·0	−0·1
80	0·0	1·0	−0·2

The estimation equation (Equation (6)) proved, in computer simulations, to be very accurate during steady state with a mean estimation error of 0.04 °C and standard deviation of 0.11 °C over the range of perfusions from 1 to 80 ml/min/100 g.

At perfusions greater than 80 ml/min/100 g there was little temperature rise between catheters and therefore temperature estimation errors were unobtainable. During transients, such as the initial heat-up of the catheters or during changes in capillary blood flow, the estimation of minimum temperature always led the actual minimum temperature in time. That is, the estimated minimum temperature would overshoot the minimum temperature, as seen in Fig. 5. However, the estimated minimum temperature did closely track the minimum temperature even during large disturbances. Fig. 12 presents the response, as modeled in computer simulations, of the bioheat equation, of the variation of the estimation/control system in the presence of a large step increase in perfusion from an initial value of 10 ml/min/100 g to 40 ml/min/100 g. Notice that the estimated temperature closely tracks the actual minimum temperature.
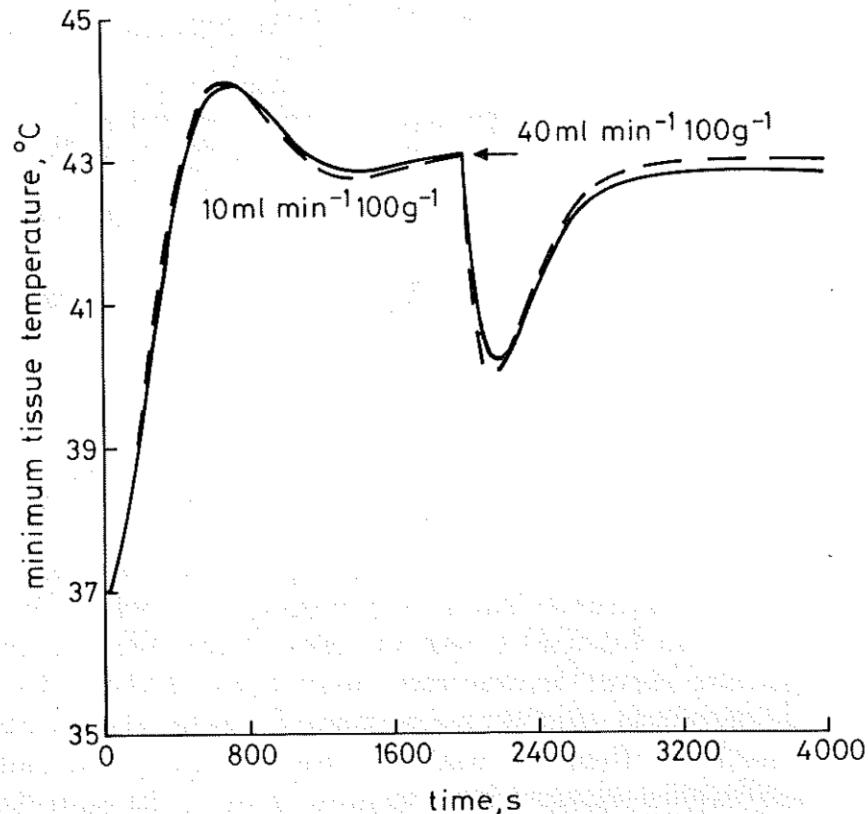
Fig. 12 The response of the closed loop system to a large disturbance in local blood flow, as modeled by the transient bioheat transfer equation, using the PI controller and the minimum temperature estimation equation. Given an initial perfusion of 10 ml/min/100 g and a minimum temperature setpoint of 43 $^{\circ}$C, the minimum temperature was controlled to the setpoint. After 2000 sec at the initial blood flow rate (10 ml/min/100 g) the perfusion was increased in step fashion to 40 ml/min/100 g. Note that after a dramatic drop in minimum temperature the minimum temperature returned to the desired setpoint without loss of stability. Also note that the estimated temperature, derived from the steady-state bioheat equation, tracked the actual temperature from the transient bioheat equation model with only small deviations. Solid curve ~ bioheat equation. Dashed curve ~ estimated equation.

3.2 Clinical data

The presented estimation/control system has been tested in nine patient treatments with no evidence of instability or large temperature estimation errors. Stability in each treatment was maintained and retrospective analysis of the temperature estimation (during steady state) revealed an average estimation error of 0.0 $^{\circ}$C with a standard deviation of 0.8 $^{\circ}$C. The design specifications were met or exceeded in all patient treatments. No patient treatment demonstrated any sign of instability in any of the nine patient treatments in which this system was employed. Specifically, the design goals included a decay ratio greater than 0.75 and a heat-up time of less

22

than 15 min. A decay ratio of greater than 0.92 was found in each patient treatment and the time required to achieve the therapeutic temperature setpoint, as determined by the estimation equation, was always less than 10 min, with an average heat-up time of 8.3 min and a standard deviation of 1.2 min.

4 Discussion

This paper presents the first report of fully closed-loop control of hyperthermia treatment of a complete tumor volume using multipoint feedback control. Previous attempts at feedback control in hyperthermia have adjusted the total or the local power delivery to achieve the desired temperature at a single selected temperature probe (MAGIN et al., 1982), and control of the entire temperature distribution was not attempted.

Because of the conceptual simplicity of conductive interstitial hyperthermia, and similarity of local temperature distributions around each heated catheter, a single algorithm can be applied to all the catheters in the array to good effect. Control of heated catheters near large blood vessels or exterior in the implanted array, although not specifically modeled, are to a large extent self-compensating, because the greater convective heat loss to a large vessel or the greater conductive heat loss from the tumor edge toward the periphery is detected as increased capillary perfusion by the estimation algorithm. This easily implemented control scheme holds promise for eliminating problems of cold spots with attendant treatment failures. Overheating of normal tissues (a major limitation with feedback control of external beam techniques) does not occur with interstitial conductive heating, because heated catheters are implanted directly into tumor tissue and blood flow outside the tumor volume provides a good heat sink, thereby keeping nearby normal tissue cool.

Hyperthermia as a treatment modality for malignant tumors does have a strong biological rationale. Heat is known to kill cells exponentially as a function of either time or temperature. However, when the treatment temperature remains near the thermal death threshold, even small temperature differences can lead to large differences in cytopathological effect (SAPARETO, 1982). Thus, effective hyperthermia treatments depend on accurate control of tissue temperatures in order to abolish cold spots (underheated volumes). The ability to estimate local minimum temperatures from clinically available data is the first, and most important, step to this technically attractive route of online, closed-loop computer control of minimum intratumoral temperatures.

We found the bioheat transfer equation to be a good model of heat transfer in biological tissues, as have other authors of previous reports (CHARNY and LEVIN, 1988; CLEGG and ROEMER, 1985; OLESON et al., 1984; PANTAZATOS and CHEN, 1978). A major practical drawback of the bioheat equation, however, is the computational time required to solve it, especially when a large number of nodes or control volumes are employed, as is necessary in the presence of steep thermal gradients characteristic of the conductive interstitial technique. To circumvent this limitation we have used offline solutions of the bioheat equation and condensed the results to produce a rapidly computable online estimation equation. These estimations provide a key to effective computer-assisted hyperthermia therapy under feedback control that promises to

minimize cold spots and associated treatment failures. By employing the estimation equation presented and ODE models of tissue heat transfers for the specific case of conductive interstitial hyperthermia, a simple and stable estimation/control system has been developed and tested. This system requires little computational overhead, yet provides a level of treatment control heretofore impossible. The accuracy and precision of these estimated temperatures seem sufficient for practical clinical use in conductive interstitial therapy of intracranial tumors.

References

ALBRITTON, E. C. (1952) Standard values in blood. W. B. Saunders Co., New York.

BAUMANN, C. K. and ZUMWALT, C. B. (1989) Volumetric interstitial hyperthermia. Assoc. Operating Room Nurses J., 50, 258-274.

CETAS, T. C., CONNER, W. G. and MANNING, M. R. (1980) Monitoring of tissue temperature during hyperthermia. Ann. NY Acad. Sci., 335, 281-297.

CHARNY, C. K. and LEVIN, R. L. (1988) Simulations of MAPA and APA heating using a whole body thermal model. IEEE Trans., BME-35, 362-370.

CLEGG, S. T. and ROEMER, R. B. (1985) A comparative evaluation of unconstrained optimization methods applied to the thermal tomography problem. J. Biomech. Eng., 107, 228-233.

COOPER, T. E. and TREZEK, G. J. (1971) Correlation of thermal properties of some human tissue with water content. Aerospace Med., 42, 24-27.

CRILE, G. (1962) Selective destruction of cancers after exposure to heat. Ann. Surg., 156, 404-407.

DEFORD, J. A., BABBS, C. F., PATEL, U. H., FEARNOT, N. E., MARCHOSKY, J. A. and MORAN, C. J. (1990) Accuracy and precision of computer simulated tissue temperatures in individual human intracranial tumors treated with interstitial hypothermia. Int. J. Hyperthermia, 6, 755-770.

DEWHIRST, M. W., SIM, D. A., SAPARETO, S. and CONNOR, W. G. (1984) Importance of minimum tumor temperature in determining early and long term responses of spontaneous canine and feline tumors to heat and radiation. Cancer Res., 44, 43-50.

EL-HAWARY, M. E. (1984) Control system engineering. Reston Publishing Co. Inc.

LEVEEN, H. H., WAPNICK, S., PICCONE, V., FALK, G. and AHMED, N. (1976) Tumor eradication by radiofrequency therapy: response in 21 patients. JAMA, 235, 2198-2220.

LEVEEN, H. H., AHMED, N., PICCONE, V. A., SHUGAAR, S. and FALK, G. (1980) Radio-frequency therapy: clinical experience. Ann. NY Acad. Sci., 335, 362-371.

LUENBERGER, D. G. (1979) Introduction to dynamic systems, theory, models, and applications. John Wiley & Sons, New York, 394-427.

MAGIN, R. L., FU, T. S., BEARD, R. E. and CAIN, C. A. (1982) Local tumor hyperthermia using a computer-controlled microwave system. Bioelectromagnetics, 3, 363-370.

MARSHALL, J. E. (1979) Control of time-delay systems. Peter Peregrinus, Stevenage, UK.

OGATA, K. (1970) Modern control engineering. Prentice-Hall, Chap. 2, 20--52; Chap. 6, 216-282; Chap. 8, 314-368.

OLESON, J. R. and CETAS, T. C. (1982). Clinical hyperthermia with RF currents. In Physical aspects of hyperthermia. NUSSBAUM, G. (Ed.), American Institute of Physics Inc., 280-305.

OLESON, J. R., BABBS, C. F. and PARKS, L. C. (1984) Improved preferential tumor hyperthermia with regional heating and systemic blood cooling: a balanced heat transfer method. Radiat. Res., 97,488-498.

PANTAZATOS, P. and CHEN, M. (1978) Computer-aided tomographic thermography: a numerical simulation. J. Bioeng., 2, 397-410.

PENNES, H. H. (1948) Analysis of tissue and arterial blood temperatures in resting forearm. J. Appl. Physiol. 1, 93-122.

PEREZ, C. A., EMAMI, B. N., KUSKE, R. R., HORNBACK, N. B., PAJAK, T. J. and KASDORF, P. (1988) Irradiation and hyperthermia in the treatment of recurrent carcinoma of the breast and chest wall: MIR and RTOG experience. In Radiation Oncology Center Scientific Report. POVILAT, C. (Ed.), Mallinckrodt Institute of Radiology, Washington University Medical Center (publishers) 278-283.

PETERSON, H. I. (1979) Tumor blood circulation: angiogenesis, vascular morphology and blood flow of experimental and human tumors. CRC Press Inc., Boca Raton, Florida, 103-114.

SAPARETO, S. A. (1982) Biology of hyperthermia in vitro. In Physical aspects of hyperthermia. NUSSBAUM, G. (Ed.), American Institute of Physics Inc., 1-19.

STORM, F. K., HARRISON, W. H., ELLIOTT, R. S. and MORTON, D. L. (1979) Normal tissue and solid tumor effects of hyperthermia in animal models and clinical trials. Cancer Res., 39, 2245-2250.